

Towards an understanding of the evolution of the scaling relations for supermassive black holes.

C. M. Booth^{1*} and Joop Schaye¹

¹*Leiden Observatory, Leiden University, PO Box 9513, 2300 RA Leiden, the Netherlands*

4 January 2011

ABSTRACT

The growth of the supermassive black holes (BHs) that reside at the centres of most galaxies is intertwined with the physical processes that drive the formation of the galaxies themselves. The evolution of the relations between the mass of the BH, m_{BH} , and the properties of its host therefore represent crucial aspects of the galaxy formation process. We use a cosmological simulation, as well as an analytical model, to investigate how and why the scaling relations for BHs evolve with cosmic time. We find that a simulation that reproduces the observed redshift zero relations between m_{BH} and the properties of its host galaxy, as well as the thermodynamic profiles of the intragroup medium, also reproduces the observed evolution in the ratio m_{BH}/m_* for massive galaxies, although the evolution of the m_{BH}/σ relation is in apparent conflict with observations. The simulation predicts that the relations between m_{BH} and the binding energies of both the galaxy and its dark matter halo do not evolve, while the ratio $m_{\text{BH}}/m_{\text{halo}}$ increases with redshift. The simple, analytic model of Booth & Schaye (2010), in which the mass of the BH is controlled by the gravitational binding energy of its host halo, quantitatively reproduces the latter two results. Finally, we can explain the evolution in the relations between m_{BH} and the mass and binding energy of the stellar component of its host galaxy for massive galaxies ($m_* \sim 10^{11} \text{ M}_\odot$) at low redshift ($z < 1$) if these galaxies grow primarily through dry mergers.

Key words: Cosmology: Theory – Galaxies: Active – Galaxies: Evolution – Galaxies: Formation – Hydrodynamics – Galaxies: Quasars: General

1 INTRODUCTION

Over the past decade it has become clear that the supermassive black holes (BHs) found at the centres of virtually all galaxies with spheroidal components, have masses that are coupled to the properties of their host galaxies (Magorrian et al. 1998; Ferrarese & Merritt 2000; Tremaine et al. 2002; Häring & Rix 2004; Hopkins et al. 2007). Additionally, there exists evidence that BH masses are coupled to the properties of the dark matter haloes in which they reside (Ferrarese 2002; Booth & Schaye 2010). Further correlations between quasar activity (e.g. Boyle & Terlevich 1998) and the evolution of the cosmic star formation rate (e.g. Madau et al. 1996) provide evidence that there exists a link between galactic star formation and accretion onto a central AGN.

It has long been recognised that the growth of BHs is likely self-regulated (Silk & Rees 1998) and that these tight correlations indicate that the growth of BHs is tightly intertwined with the physical processes that drive galaxy for-

mation. However, despite a wide variety of theoretical and observational studies, the origin of these relations is still debated. The study of the evolution of the BH scaling relations therefore represents a crucial aspect of the galaxy formation process that may provide us with additional clues regarding the physical processes that give rise to the BH scaling relations.

Addressing these questions observationally is challenging. Due to their extremely high luminosities, bright quasars provide a promising route to measuring BH masses at high redshift through the widths of low-ionization lines that are associated with the broad-line region close to the BH and using the assumption of virial equilibrium (e.g. Vestergaard 2002). It has, however, been claimed that this procedure systematically underestimates BH masses (Jarvis & McLure 2002). Measuring galaxy masses for these objects is very difficult as the BH outshines the galaxy by a large factor (see e.g. the discussion in Merloni et al. 2010). Since AGN surveys are biased towards more massive black holes, selection effects also need to be taken into account (e.g. Shen & Kelly 2009; Bennert et al. 2010), which can make it difficult to distinguish between evolution in the normalization and in the

* E-mail: booth@strw.leidenuniv.nl (CMB)

scatter in the scaling relations (Lauer et al. 2007). In spite of these difficulties, measurements of the BH scaling relations have been made as far out as redshift three.

McLure et al. (2006) found that the BHs associated with radio loud AGN residing in galaxies of a given stellar mass are a factor of four more massive at redshift two than in the local Universe. Decarli et al. (2010) studied the CIV line associated with the quasar broad line region in R-band selected hosts at both redshifts zero and three and found that BHs are typically a factor of seven more massive at high redshift for a given galaxy mass. These results are consistent with other observational studies (Walter et al. 2004; Peng et al. 2006a,b; Merloni et al. 2010; Greene et al. 2010; Bennert et al. 2010). Taken together, these papers suggest an emerging consensus that at higher redshift BHs in hosts of a given mass are systematically more massive than in the local Universe, although see Jahnke et al. (2009) for one study that finds no significant evolution.

The evolution of the relation between BH mass, m_{BH} , and stellar velocity dispersion, σ_* , has been studied utilising the width of the OIII line as a proxy for stellar velocity dispersion (Nelson & Whittle 1996). These studies suggest that the $m_{\text{BH}} - \sigma_*$ relation either does not evolve (Shields et al. 2003; Gaskell 2009), or does so weakly, with BHs $\sim 0.1 - 0.3$ dex more massive at $z = 1$ (Salviander et al. 2006; Gu et al. 2009; Woo et al. 2008; Treu et al. 2007).

The evolution of the BH scaling relations has also been studied using numerical simulations (e.g. Robertson et al. 2006; Johansson et al. 2009) and semi-analytic models (e.g. Malbon et al. 2007; Lemastra et al. 2010; Kisaka & Kojima 2010). Robertson et al. (2006) employed simulations of idealised galaxy mergers, initialised to have properties typical of merger progenitors at various redshifts, to construct the relation between galaxy stellar mass, m_* , and σ_* as a function of redshift and found that, at a given value of σ_* , the corresponding m_{BH} decreases mildly with increasing redshift. At $z = 1$ the simulations of Di Matteo et al. (2008) have BHs that lie slightly above the $z = 0$ normalization of the $m_{\text{BH}} - \sigma$ relation. However, these simulations were stopped at $z = 1$ and so cannot inform us about the evolution of the $m_{\text{BH}} - \sigma_*$ toward lower redshift. However, for $z > 1$ they predict a weak evolution in the $m_{\text{BH}} - \sigma_*$ relation such that at higher redshift galaxies of a given velocity dispersion contain slightly less massive BHs. Johansson et al. (2009) employed similar numerical techniques to argue that it is unlikely that BHs are able to form significantly before their host bulges. Semi-analytic models that reproduce many redshift zero properties of galaxies also predict that, at a fixed σ_* , BH masses decrease with increasing redshift (Malbon et al. 2007). These theoretical models thus predict evolutionary trends that go in the opposite direction to those inferred from observations. Finally, the models of Hopkins et al. (2009) predict that, at a fixed stellar velocity dispersion, BH masses at higher redshift are either the same (for $m_{\text{BH}} \sim 10^8 M_\odot$) or slightly more massive (for $m_{\text{BH}} > 10^8 M_\odot$) at fixed σ_* than their redshift zero counterparts, in agreement with observation.

On the other hand, the relation between BH mass and galaxy bulge mass shows a positive evolution in both semi-analytic models (Malbon et al. 2007; Hopkins et al. 2009) and numerical simulations (Di Matteo et al. 2008), the magnitude of which is comparable to that observed. The larger

spread in the predictions for the evolution of the $m_{\text{BH}} - \sigma_*$ relation may reflect that it is more difficult to predict velocity dispersions, which depend on both mass and size, than it is to predict masses.

In Booth & Schaye (2009, hereafter BS09) we presented self-consistent, hydrodynamical simulations of the co-evolution of the BH and galaxy populations that reproduce the redshift zero BH scaling relations. These same simulations also match group temperature, entropy and metallicity profiles, as well as the stellar masses and age distributions of brightest group galaxies (McCarthy et al. 2010). In Booth & Schaye (2010) (hereafter BS10) we used the same simulations, as well as an analytic model, to demonstrate that m_{BH} is determined by the mass of the dark matter (DM) halo with a secondary dependence on the halo concentration, of the form that would be expected if the halo binding energy were the fundamental property that controls the mass of the BH. In the present work we use the same models to investigate why and how the BH scaling relations evolve for massive galaxies.

This paper is organised as follows. In Sec. 2 we summarise the numerical methods employed in this study and the simulation analysed. In Sec. 3 we present predictions for the evolution of the BH scaling relations and compare them to observations. We find that the evolution in the $m_{\text{BH}} - m_*$ relation predicted by the simulations is in excellent agreement with the observations, while the measured weak evolution in the $m_{\text{BH}} - \sigma$ relation is in apparent disagreement, and predict that while BH mass increases with redshift for fixed halo mass, the relations between m_{BH} and the binding energies of both the host galaxies and DM haloes do not evolve. We demonstrate in 4 that the analytic description in which m_{BH} is coupled to the DM halo binding energy can reproduce the evolution of the relation between BH and halo mass. Furthermore, we show that the evolution in the relations between the BH and the stellar mass and binding energy can be understood in terms of the more fundamental relation with the binding energy of the dark halo and the growth of massive galaxies through dry mergers. Finally, we summarise our main conclusions in Sec. 5.

2 NUMERICAL METHOD

We have carried out a cosmological simulation using a significantly extended version of the parallel PMTree-Smoothed Particle Hydrodynamics (SPH) code GADGET III (last described in Springel 2005). The simulation and code are described in detail in BS09, we provide only a brief summary here. In addition to hydrodynamic forces, we treat star formation (Schaye & Dalla Vecchia 2008), supernova feedback (Dalla Vecchia & Schaye 2008), radiative cooling (Wiersma et al. 2009a), chemodynamics (Wiersma et al. 2009b) and black hole accretion and feedback (BS09, Springel et al. 2005). We summarise in Sec. 2.1 the essential features of the BH model.

The properties of central galaxies and DM haloes are calculated by first identifying the most gravitationally bound particle in each DM halo using the algorithm SUBFIND (Springel et al. 2001; Dolag et al. 2009), which is then considered the halo centre. All stars within a radius of $0.15 r_{\text{halo}}$ are then assigned to the central galaxy. We note that our

conclusions are insensitive to the exact choice for this radius, and whether we use a fixed physical value or a fixed fraction of the halo virial radius. As long as the sphere encloses the central object, our results are insensitive to this choice. Halo mass, m_{halo} , is calculated as the total mass enclosed within a sphere, centred on the most bound particle in the halo, that has a mean density of 200 times the mean density of the Universe and the virial radius r_{halo} is the radius of this sphere. Because it is not expected that the same physics holds for both the central galaxy of a halo and its satellites, which are expected to rapidly have their gas supply stripped when they become satellites, our analysis is restricted to BHs identified as residing in the central galaxy in a DM halo, defined as the galaxy closest to the centre of the DM potential well of each halo.

2.1 The black hole model

Seed BHs of mass $m_{\text{seed}} = 10^{-3} m_g \approx 10^5 M_\odot$ – where m_g is the simulation gas particle mass – are placed into every DM halo that contains more than 100 DM particles (which corresponds to a DM halo mass of $4.1 \times 10^{10} M_\odot/h$) and does not already contain a BH particle. Haloes are identified by regularly running a friends-of-friends group finder during the simulation. After forming, BHs grow by two processes: accretion of ambient gas and mergers. Gas accretion occurs at the minimum of the Eddington rate, $\dot{m}_{\text{Edd}} = 4\pi G m_{\text{BH}} m_p / \epsilon_r \sigma_{\text{T}} c$ and $\dot{m}_{\text{accr}} = \alpha 4\pi G^2 m_{\text{BH}}^2 \rho / (c_s^2 + v^2)^{3/2}$, where m_p is the proton mass, σ_{T} is the Thomson cross-section, ϵ_r is the radiative efficiency of the BH, c is the speed of light, c_s and ρ are the sound speed and gas density of the local medium, v is the velocity of the BH relative to the ambient medium, and α is a dimensionless efficiency parameter. The parameter α accounts for the fact that our simulations possess neither the necessary resolution nor the physics to accurately model accretion onto a BH on small scales. Note that for $\alpha = 1$ this accretion rate reduces to the so called Bondi-Hoyle (Bondi & Hoyle 1944) rate.

As long as we resolve the scales and physics relevant to Bondi-Hoyle accretion, we should set $\alpha = 1$. If a simulation resolves the Jeans scales in the accreting gas, then it will also resolve the scales relevant for Bondi-Hoyle accretion onto any BH larger than the simulation mass resolution (BS09). We therefore generally set α equal to unity. However, this argument breaks down in the presence of a multi-phase interstellar medium, because our simulations do not resolve the properties of the cold, molecular phase, and as such the accretion rate may be orders of magnitude higher than the Bondi-Hoyle rate predicted by our simulations for star-forming gas. We therefore use a power-law scaling of the accretion efficiency such that $\alpha = (n_{\text{H}}/n_{\text{H}}^*)^\beta$ in star-forming gas, where $n_{\text{H}}^* = 0.1 \text{ cm}^{-3}$ is the critical density for the formation of a cold, star-forming gas phase. The parameter β is a free parameter in our simulations. We set $\beta = 2$, but note that the results shown here are insensitive to changes in this parameter when $\beta \gtrsim 2$. We note that we do not resolve the Bondi radius of BHs less massive than the particle mass in our simulations, and that for BHs with $m_{\text{BH}} \sim m_g$ the Bondi radius is unresolved unless the density is low or the temperature high. Our choice of $\alpha = 1$ therefore provides an underestimate of the true accretion rate in these regimes. However, even setting $\alpha = 100$ for all densi-

ties gives very similar results (Booth & Schaye 2009). This is because all BHs accrete almost all of their mass in short, (near) Eddington-limited bursts of accretion and thus that our treatment of accretion in low-density environments is less important. The accretion model in high-density environments is necessarily very crude, but we note that our results are insensitive to the details of the accretion model as long as α is sufficiently large that the BHs become more massive than observed in the absence of feedback and if two reasonable conditions are met that are necessary for self-regulation to be possible. Firstly, the BH accretion rate must increase with increasing density, and secondly it must increase with BH mass (see BS09).

Energy feedback is implemented by allowing BHs to inject a fixed fraction of the rest mass energy of the gas they accrete into the surrounding medium. The energy deposition rate is given by

$$\dot{E} = \epsilon_f \epsilon_r \dot{m}_{\text{accr}} c^2 = \frac{\epsilon_f \epsilon_r}{1 - \epsilon_r} \dot{m}_{\text{BH}} c^2, \quad (1)$$

where \dot{m}_{accr} is the rate at which the BH is accreting gas, and \dot{m}_{BH} is the rate of BH mass growth.

We set ϵ_r to be 0.1, the mean value for radiatively efficient accretion onto a Schwarzschild BH (Shakura & Sunyaev 1973) and use $\epsilon_f = 0.15$ as our fiducial value. It was shown in BS09 that, for $\epsilon_f = 0.15$, this simulation reproduces the observed redshift zero $m_{\text{BH}} - m_*$ and $m_{\text{BH}} - \sigma_*$ relations. Energy is returned to the surroundings of the BH ‘thermally’, by increasing the temperature of N_{heat} of the BH’s neighbouring SPH particles by at least ΔT_{min} . A BH performs no heating until it has built up enough of an energy reservoir to heat by this amount. Imposing a minimum temperature increase ensures that the radiative cooling time is sufficiently long for the feedback to be effective. We set $N_{\text{heat}} = 1$ and $\Delta T_{\text{min}} = 10^8 \text{ K}$ but the results are insensitive to the exact values of these parameters (see BS09).

2.2 The cosmological simulation

The simulation employed in the current work uses a cubic box of size 50 comoving Mpc/h and assumes periodic boundary conditions. The simulation contains 256^3 particles of both gas and collisionless cold DM and is evolved down to redshift zero. The DM and initial baryonic particle masses are $4.1 \times 10^8 M_\odot/h$ and $8.7 \times 10^7 M_\odot/h$, respectively. Comoving gravitational softenings are set to 1/25 of the mean interparticle separation down to $z = 2.91$, below which they switch to a fixed proper scale of 2 kpc/h. The simulation employed in this study was previously also analysed as the fiducial simulation in BS09 and BS10.

Comparison of the simulation employed in this study to an otherwise identical one with eight (two) times lower mass (spatial) resolution informs us in what mass and redshift range the relations between m_{BH} and galaxy and halo properties are numerically converged. The relation between m_{BH} and both m_* and m_{halo} is numerically converged up to redshift two for all haloes with $m_{\text{BH}} > 10 m_{\text{seed}}$. Measurements of stellar velocity dispersion are, however, only converged for $z < 1$ and $m_{\text{BH}} > 10^2 m_{\text{seed}}$. We will only give results for redshifts and BH masses for which the results are converged with respect to numerical resolution.

We note that these simulations do not resolve the scales

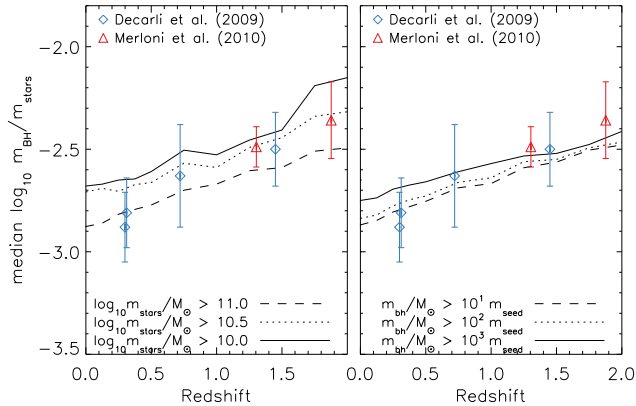


Figure 1. The median m_{BH}/m_* ratio as a function of redshift for galaxies of different stellar masses (*left panel*) and for BHs above a given mass (*right panel*) predicted by the cosmological simulation. The points with error bars show the measurements of Merloni et al. (2010, red triangles) for a sample of galaxies in the mass range $10.5 < \log(m_*/M_\odot) < 11.5$ and Decarli et al. (2010, blue diamonds) for a sample of galaxies with typical stellar masses $\sim 10^{11} M_\odot$. We show a number of different mass cuts for the simulation results to demonstrate that the results are insensitive to the particular mass cut chosen. Both the simulations and observations in this plot show the *total* stellar mass of the galaxies. The simulation predicts that the median m_{BH}/m_* ratio increases with redshift. The predictions are in excellent agreement with the observations, regardless of the particular mass cut made.

on which the BH is the gravitationally dominant component in the galaxy and so cannot be used to study BH self-regulation on the smallest scales. However, the simulations do have sufficient resolution for baryons to be gravitationally dominant in the centres of haloes. We cannot conclusively rule out that if we increased our mass resolution significantly and used more sophisticated sub-grid models that the BH would self-regulate on different scales. However, suggestively, in Booth & Schaye (2010) we verified that in simulations with a spatial resolution of $0.5 \text{ kpc}/h$ that, at $z = 2$, the BH masses scale in the same way as in the lower-resolution simulations.

3 SIMULATION RESULTS

3.1 The evolving relations between black holes and galaxies

Fig. 1 compares the predicted evolution of the median m_{BH}/m_* ratio for different minimum stellar (left panel) and BH (right panel) masses with observations of AGN in galaxies with $m_* \sim 10^{11} M_\odot$. The m_{BH}/m_* ratio increases with redshift, in close agreement with observations (Merloni et al. 2010; Decarli et al. 2010). At redshift zero this agreement is unsurprising because the efficiency of AGN feedback in the simulation was tuned to reproduce the normalisation of the $z = 0$ BH scaling relations. The agreement at higher redshift represents, however, a non-trivial prediction of a model in which BHs self-regulate their accretion through the coupling of a small fraction of the radiative energy to the ambient medium.

In Table 1 we show the predicted evolution up to $z =$

Table 1. Evolution of the normalisation of the power-law relations between BH mass and the properties of its host. The sample includes all galaxies that contain a BH with $m_{\text{BH}} > 10^2 m_{\text{seed}} \approx 10^7 M_\odot$, corresponding to 162 (132) haloes at $z = 0$ ($z = 1$). The median BH, stellar, and halo mass are $10^{7.6}$, $10^{10.6}$, and $10^{12.8} M_\odot$, respectively. The central column gives the median change in $\log_{10} m_{\text{BH}}$ at redshift one relative to $z = 0$ for fixed values of the quantity listed in the left column. The right column shows the slope, α_s , of the best fit power-law describing the rate of evolution of the scaling relation (Eq. 2) over the redshift range $0 - 1$. From top to bottom, we consider evolution of m_{BH} for fixed stellar mass, halo mass, central stellar velocity dispersion, galaxy binding energy ($m_* \sigma_*^2$), and halo binding energy (Eq. 3). Errors are calculated from 10^3 bootstrap resamplings of the data.

Variable	$\Delta \log_{10} \frac{m_{\text{BH}}(z=1)}{m_{\text{BH}}(z=0)}$	α_s
m_*	0.20 ± 0.05	0.52 ± 0.05
m_{halo}	0.23 ± 0.03	0.65 ± 0.06
σ_*	-0.09 ± 0.04	-0.32 ± 0.05
U_*	0.02 ± 0.03	0.05 ± 0.06
U_{halo}	0.01 ± 0.03	0.03 ± 0.05

1 of the amplitude of the relations between m_{BH} and the masses, velocity dispersions and binding energies of both the host galaxies and the host DM haloes. The central column gives $\log_{10} m_{\text{BH}}(z = 1) - \log_{10} m_{\text{BH}}(z = 0)$, calculated by fitting power-law relations under the assumption that the slopes of the scaling relations do not evolve, which is a good approximation in the redshift range studied here¹. The right-most column of Table 1 gives the slope, α_s , of the power-law evolution in the amplitude of each scaling relation

$$\frac{m_{\text{BH}}}{X^{n_0}} \propto (1+z)^{\alpha_s}, \quad (2)$$

where X is one of the variables listed in the left column, and n_0 is the slope of the $m_{\text{BH}} - X$ relation at $z = 0$. We find that $\alpha_s = 0.52 \pm 0.05$ for the $m_{\text{BH}} - m_*$ relation, in good agreement with Di Matteo et al. (2008), who found $\alpha_s = 0.5$.

The evolution of the $m_{\text{BH}} - \sigma_*$ relation is smaller but significant, with $\alpha_s = -0.32 \pm 0.05$. This is in apparent disagreement with various observational studies that either infer a positive (Salviander et al. 2006; Treu et al. 2007; Woo et al. 2008; Gu et al. 2009) or negligible (Shields et al. 2003; Gaskell 2009) evolution in the normalisation of the $m_{\text{BH}} - \sigma_*$ relation. The predicted evolution does, however, agree with other simulation studies (Robertson et al. 2006) and semi-analytic models (Malbon et al. 2007). Taken together, the simulation predicts that the $m_{\text{BH}} - m_*$ and

¹ At $z = 0$ ($z = 1$) the slope of the relation between m_{BH} and U_{halo} is 1.01 ± 0.14 (0.96 ± 0.17) and the slope of the relation between m_{BH} and U_* is 0.93 ± 0.07 (0.96 ± 0.09), consistent with the $z = 0$ observational results of Feoli & Mele (2007) and Feoli et al. (2010). At all redshifts these slopes are consistent with unity. The slopes of the relations between m_{BH} and m_* , σ_* and m_{halo} are 1.16 ± 0.06 (1.2 ± 0.2), 4.6 ± 0.8 (4.4 ± 0.8) and 1.5 ± 0.2 (1.5 ± 0.3). There is thus no evidence for evolution in any of the slopes, which agrees with the results of Robertson et al. (2006) for the $m_{\text{BH}} - \sigma_*$ relation and with Di Matteo et al. (2008) for the $m_{\text{BH}} - m_*$ relation. The slopes of the $z = 0$ relations are consistent with observations (Häring & Rix 2004; Tremaine et al. 2002; Bandara et al. 2009).

$m_{\text{BH}} - \sigma_*$ relations evolve such that the relation between m_{BH} and stellar binding energy ($\propto m_* \sigma_*^2$) is independent of redshift ($\alpha_s = 0.05 \pm 0.06$).

It is tempting to conclude from the finding that the ratio $m_{\text{BH}}/(m_* \sigma_*^2)$ does not evolve that the BH mass is determined by the binding energy of the galaxy. However, we demonstrated explicitly in BS10 that the BH mass is instead controlled by the binding energy of the DM halo. This implies that the binding energy of the galaxy tracks the binding energy of the halo, which we will confirm and explain below.

3.2 The evolving relations between black holes and dark matter haloes

We now turn our attention to the relations between the mass of the BH and the DM halo in which it resides. In BS10 we argued that a BH grows until it has injected an amount of energy into its surroundings that scales with the binding energy of its host DM halo. We therefore do not expect the $m_{\text{BH}} - U_{\text{halo}}$ relation to evolve. Indeed, in the simulation the amplitude of this relation is independent of redshift, with $\alpha_s = 0.03 \pm 0.05$, as would be expected for a fundamental link between m_{BH} and the binding energy of the host DM halo.

We do, however, expect the relation between m_{BH} and m_{halo} to evolve. At higher redshift, haloes of a given mass are more compact than their redshift zero counterparts and are thus more strongly gravitationally bound. This means that, at a fixed halo mass, more energy is required to eject gas from haloes at high redshift and in order to self-regulate, BHs must grow to be more massive. Fig. 2 shows the normalisation of the $m_{\text{BH}} - m_{\text{halo}}$ relation as a function of redshift and confirms that the simulation predicts the amplitude of this relation to increase with redshift (red, dashed curve), with $\alpha_s = 0.65 \pm 0.06$.

4 EXPLAINING THE EVOLUTION

As we already noted, the idea that the binding energy of the dark halo controls the mass of the BH explains our finding that the $m_{\text{BH}} - U_{\text{halo}}$ relation is independent of redshift. We will now show that the analytic model of BS10 also reproduces the evolution of the $m_{\text{BH}} - m_{\text{halo}}$ relation and that it can explain the observed evolution in the scaling relations with the stellar properties if the observed galaxies evolve predominantly through dry mergers, as predicted by the simulation.

4.1 The $m_{\text{BH}} - m_{\text{halo}}$ relation

If the energy injected by a BH is proportional to the halo gravitational binding energy, U_{halo} , then, for a DM halo with an NFW (Navarro et al. 1997) density profile (BS10)

$$m_{\text{BH}} \propto U_{\text{halo}} \propto \frac{m_{\text{halo}}^2}{r_{\text{halo}}} \propto f(c, x)(1+z)m_{\text{halo}}^{5/3}, \quad (3)$$

where m_{halo} is the halo mass, $c(m_{\text{halo}}, z)$ is the halo concentration, x is defined to be $x \equiv r_{\text{ej}}/r_{\text{halo}}$, r_{ej} is the physical scale on which BH self-regulation takes place, and $f(c, x)$ is

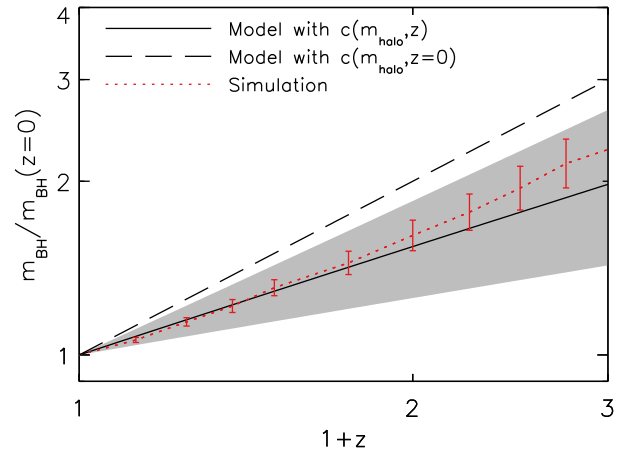


Figure 2. Predicted evolution of the normalisation of the $m_{\text{BH}} - m_{\text{halo}}$ relation. The red, dotted curve shows the median evolution predicted by the cosmological simulation when all BHs for which both BH and halo properties are well resolved ($m_{\text{BH}} > 10^2 m_{\text{seed}}$) are included. The grey region represents the allowed range in evolution predicted by the analytic model of BS10, which assumes that the BH mass is controlled by the binding energy of the DM halo. The binding energy of an NFW halo depends on mass, redshift, concentration (which itself depends on both mass and redshift) and on the radius, r_{ej} , at which it is evaluated. The grey region corresponds to $r_{\text{ej}}/r_{\text{halo}} = 0.1 - 1.0$ (bottom to top) and the solid black line to $r_{\text{ej}} = 0.22 r_{\text{halo}}$, the value for which we predict $m_{\text{BH}} \propto m_{\text{halo}}^{1.55}$ at $z = 0$, in accord with both observations (Bandara et al. 2009) and simulation (BS10). For comparison, the black dashed line shows the evolution that our analytic model would have predicted if we had ignored the evolution of the $c(m_{\text{halo}})$ relation. At all redshifts the normalisation of the simulated $m_{\text{BH}} - m_{\text{halo}}$ relation (red, dotted curve) agrees with that predicted by the analytic model based on the assumption that the fundamental relation is between BH mass and the binding energy of the DM halo.

the function

$$f(c, x) = \frac{c}{(\ln(1+c) - c/(1+c))^2} \times \left(1 - \frac{1}{(1+cx)^2} - \frac{2 \ln(1+cx)}{1+cx} \right). \quad (4)$$

Simulations have shown that c is a function of both redshift and halo mass, and scales approximately as² (Duffy et al. 2008)

$$c \propto m_{\text{halo}}^{-0.1} (1+z)^{-0.5}. \quad (5)$$

Combining Eqs. 3-5, BS10 found the slope of the $m_{\text{BH}} - m_{\text{halo}}$ relation to be weakly dependent on r_{ej} . At $z = 0$ it varies from $n_0 = 1.50$ for $x = 0.1$ to $n_0 = 1.61$ for $x = 1.0$. In order to exactly match the slope of 1.55 that is both observed (Bandara et al. 2009 find 1.55 ± 0.31) and predicted by the

² Note that the slope of the power-law dependence of concentration on redshift depends on the halo definition used (Duffy et al. 2008).

simulations (BS10 find 1.55 ± 0.05 for the same simulation as is analyzed here³), we would need to use $x = 0.22$.

By using an NFW density profile and Eq. (5), we have implicitly assumed that the dark matter profile is well described by the results obtained from simulations that include only dark matter. Duffy et al. (2010) have recently shown that, on the scales of interest here, the back-reaction of the baryons onto the dark matter is in fact very small if feedback from AGN is included, as required to reproduce the observed stellar and gas properties of groups of galaxies (McCarthy et al. 2010; Puchwein et al. 2008; Fabjan et al. 2010; Duffy et al. 2010).

If, as argued in BS10, the BH mass is controlled by the DM halo binding energy, then we expect the $m_{\text{BH}} - m_{\text{halo}}$ relation to evolve because the halo binding energy depends not only on halo mass, but also on the virial radius and concentration, both of which vary with redshift for a fixed halo mass.

If the $c - m_{\text{halo}}$ relation did not evolve, then we would expect $m_{\text{BH}}(m_{\text{halo}}) \propto (1+z)$ (Eq. 3). However, because halo concentration decreases with redshift (Eq. 5) we expect the actual evolution of the $m_{\text{BH}} - m_{\text{halo}}$ relation to be weaker, i.e. $\alpha_s < 1$. The resulting relation between BH mass and DM halo binding energy predicts that, at a given m_{halo} , m_{BH} increases with redshift and that by $z = 2$ BHs are between 1.5 (for $r_{\text{ej}}/r_{\text{halo}} = 0.1$) and 2.6 (for $r_{\text{ej}}/r_{\text{halo}} = 1.0$) times more massive than at redshift zero. For our fiducial radius of self-regulation of $x = 0.22$, BHs are 2.1 times more massive, in excellent agreement with the simulation prediction of $\alpha_s = 0.65 \pm 0.06$ (Table 1).

The evolution predicted by Eqs. 3-5 is shown in Fig. 2. The grey shaded region outlines the analytic prediction for the evolution in BH mass over the range $r_{\text{ej}}/r_{\text{halo}} = 0.1 - 1.0$ and the solid black line shows the prediction for $r_{\text{ej}}/r_{\text{halo}} = 0.22$ (the value that reproduces the slope of the redshift zero $m_{\text{BH}} - m_{\text{halo}}$ relation). The red, dotted curve shows the simulation prediction for the evolution of the $m_{\text{BH}} - m_{\text{halo}}$ relation, including all BHs with $m_{\text{BH}} > 10^2 m_{\text{seed}}$. At all redshifts the normalisation of the simulated $m_{\text{BH}} - m_{\text{halo}}$ relation is compatible with that predicted by the analytic model. For comparison, the dashed, black line shows the predicted evolution of the $m_{\text{BH}} - m_{\text{halo}}$ relation if $c(m_{\text{halo}})$ were independent of redshift. The analytic model can only reproduce the simulation result if the evolution of the concentration-mass relation is taken into account.

The evolution of the $m_{\text{BH}} - m_{\text{halo}}$ relation thus provides additional evidence for the idea that the masses of BHs are determined by the binding energies of the haloes in which they reside.

4.2 The relations between m_{BH} and galaxy stellar properties

Considering now only the stellar masses for which the evolution has been measured observationally ($m_* \sim 10^{11} M_\odot$) and the redshift range for which all of the stellar and BH properties of the galaxies are converged numerically ($z < 1$), we ask if we can explain how the relations between BH mass

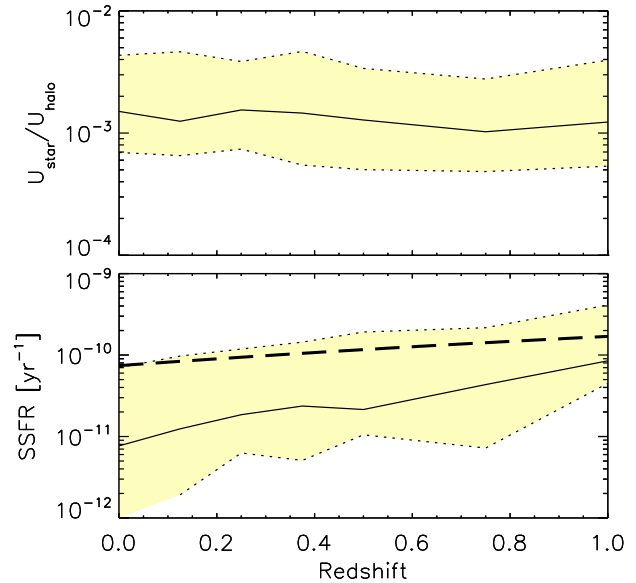


Figure 3. Galaxy properties as a function of redshift for $m_* \approx 10^{11} M_\odot$ (at each redshift we selected the 20 galaxies with stellar masses closest to this value). The yellow shaded region shows the area that contains the 25th to 75th percentiles of the data and the black, solid curve shows the median. The top panel shows the ratio of stellar to halo binding energy and the bottom panel shows the specific star formation rate ($\text{SSFR} \equiv \dot{m}_*/m_*$). The dashed line in the bottom panel shows the inverse of the age of the Universe. Galaxies with SSFRs below this line may be considered passive.

and galaxy stellar properties evolve. BS10 showed that the BH mass is determined by the binding energy of the DM halo, which explains why the $m_{\text{BH}} - U_{\text{halo}}$ relation does not evolve. We find that the $m_{\text{BH}} - U_*$ relation also does not evolve, implying that, over the range of redshifts and masses investigated here, $U_* \propto U_{\text{halo}}$. The top panel of Fig. 3 confirms that this is indeed the case in our simulation.

For the binding energy of the galaxy to track that of the halo, we require the two to grow through the same mechanism. This condition is met if the galaxies grow primarily through dry mergers. In the absence of significant in-situ star formation, both the stellar component, which is predominantly spheroidal for massive galaxies, and the DM halo are collisionless systems and are therefore expected to evolve in a similar manner.

The bottom panel of Fig. 3 shows that at $z \ll 1$ the specific star formation rates ($\text{SSFR} \equiv \dot{m}_s/m_*$) of galaxies with $m_* \sim 10^{11} M_\odot$ are significantly lower than the inverse of the Hubble time, $1/t_H$, implying that the galaxies are indeed not growing significantly via in-situ star-formation, in agreement with various observations (e.g. Schawinski et al. 2006; van der Wel et al. 2009; Bezanson et al. 2009; van Dokkum et al. 2010). The analysis in Fig. 3 was carried out for galaxies at a fixed stellar mass, but the same results hold if we trace individual galaxies through time. While the stellar masses of the most massive $z = 0$ galaxies grew on average by a factor 2.65 since $z = 1$, the fraction of stars in the redshift zero objects with birth redshifts below $z = 1$ is, on average, only 15%.

Merloni et al. (2010) studied the evolution of the BH

³ We quoted a slope of 1.5 ± 0.2 . Our error bar is greater because BS10 used $m_{\text{BH}} > 10m_{\text{seed}}$ whereas we require $m_{\text{BH}} > 100m_{\text{seed}}$.

scaling relation in the redshift range $1 < z < 2.2$, and found that at $z = 1$ a large fraction of galaxies would be identified as star-forming. This is consistent with our results as the SSFRs of our galaxy sample are increasing with increasing redshift so that a significant fraction of them would be identified as star-forming at $z \approx 1$. The fraction would be even higher if we had required the galaxies to contain active AGN, as is the case for the objects selected in the observations, because AGN activity is typically accompanied by a temporary increase in the star formation rate.

One might naively think that the $m_{\text{BH}} - m_*$ relation should not evolve at all if the galaxies grew predominantly through dry mergers. However, the progenitors of galaxies with $m_* \sim 10^{11} M_\odot$ at $z = 0$ typically formed their stars and grew their BHs later than the progenitors of galaxies that already have the same stellar mass at $z = 1$. Because the progenitors of higher redshifts galaxies formed earlier, they have higher binding energies and thus greater BH masses relative to their halo masses. Thus, even if $m_* \sim 10^{11} M_\odot$ galaxies are growing predominantly by dry mergers at both redshifts, they may have different BH masses. Observe, however, that the evolution in the $m_{\text{BH}} - m_*$ relation that we predict for these massive galaxies is only mild (about 0.2 dex; see Fig. 1) and that in situ star formation thus become important for $z \gtrsim 1$ (see Fig. 3).

If the ratio of the stellar to halo binding energies remains constant, we can write

$$m_{\text{BH}} \propto U_{\text{halo}} \propto U_* \propto m_* \sigma_*^2. \quad (6)$$

To explain the evolution of m_{BH}/m_* that is observed for $m_* \sim 10^{11} M_\odot$, and which the simulation reproduces, we need to know how the $m_* - \sigma_*$ relation evolves for such galaxies.

Measurements of the evolution of the $m_* - \sigma_*$ relation have so far only been undertaken for a small number of objects. Cappellari et al. (2009) presented stacked observations of seven galaxies with $m_* \sim 10^{11} M_\odot$ in the redshift range $1.6 < z < 2.0$ and found that these galaxies typically have the same σ_* as the very highest velocity dispersion early-type galaxies of the same mass in the local Universe. This is in agreement with observations showing that galaxies of a given stellar mass are more compact at higher redshifts (see e.g. Williams et al. 2010). Indeed, for early-type galaxies with stellar masses $\sim 10^{11} M_\odot$ Cenarro & Trujillo (2009) find that typical velocity dispersions decrease from ≈ 240 km/s at $z = 1.6$ to ≈ 180 km/s at $z = 0$, which implies $\sigma_* \propto (1+z)^{0.3}$. Combined with Eq. (6) this yields $m_{\text{BH}}/m_* \propto (1+z)^{0.6}$, in good agreement with the $\alpha_s \approx 0.5$ that is observed for galaxies of this mass.

5 CONCLUSIONS

We have used a self-consistent cosmological simulation that reproduces the observed redshift zero relations between m_{BH} and both galaxy and halo properties (as well as the thermodynamic profiles of the intragroup medium) to investigate how, and why, these relations evolve through time.

The relation between BH mass and host galaxy mass predicted by the simulation is consistent with available observations at $z < 2$, which are currently confined to $m_* \sim 10^{11} M_\odot$ galaxies. For such galaxies we predict that the ratio

$m_{\text{BH}}/m_* \propto (1+z)^{\alpha_s}$, with $\alpha_s \approx 0.5$, and $m_{\text{BH}}/\sigma_*^4 \propto (1+z)^{\alpha_s}$ with $\alpha_s \approx -0.3$, in apparent conflict with recent observations. The ratio between the BH mass and the binding energy of the dark halo is independent of redshift, in agreement with BS10 who argued that the BH mass is controlled by the halo binding energy. The simple analytic model of BS10, in which the BH mass is assumed to scale in proportion to the binding energy of the dark halo, not only reproduces the simulated redshift zero $m_{\text{BH}} - m_{\text{halo}}$ relation, but also its evolution. For a fixed halo mass BHs are more massive at higher redshift because the haloes are more compact and thus more tightly bound. Assuming an NFW halo density profile and the evolution of the halo concentration-mass relation predicted by simulations, the model can quantitatively account for the predicted evolution.

The simulation predicts that the ratio between the BH mass and the binding energy of the stellar component of the galaxy is also independent of redshift (at least for $m_* \sim 10^{11} M_\odot$ and $z < 1$), even though BS10 demonstrated explicitly that the correlations between BH mass and stellar properties are not fundamental. This result is, however, consistent with a picture in which massive galaxies grow primarily through dry mergers at low redshift, which we showed to be the case in the simulation. Combined with the observed evolution in the $m_* - \sigma_*$ relation, this idea can quantitatively account for the evolution in the $m_{\text{BH}} - m_*$ relation.

One interesting implication of this scenario is that the evolution of the relations between BHs and the properties of their host galaxies may differ for galaxies that do not grow predominantly through dry mergers, as would be expected for lower masses and at higher redshifts. We will investigate this further in a future work, employing higher resolution simulations.

ACKNOWLEDGEMENTS

We would like to thank Marcel Haas for a careful reading of the manuscript and the anonymous referee for comments that improved its clarity. The simulations presented here were run on the Cosmology Machine at the Institute for Computational Cosmology in Durham as part of the Virgo Consortium research programme, on Stella, the LO-FAR BlueGene/L system in Groningen, and on Huygens, the Dutch national supercomputer. This work was supported by an NWO Vidi grant.

REFERENCES

- Bandara K., Crampton D., Simard L., 2009, ApJ, 704, 1135
- Bennert V. N., Treu T., Woo J., Malkan M. A., Le Bris A., Auger M. W., Gallagher S., Blandford R. D., 2010, ApJ, 708, 1507
- Bezanson R., van Dokkum P. G., Tal T., Marchesini D., Kriek M., Franx M., Coppi P., 2009, ApJ, 697, 1290
- Bondi H., Hoyle F., 1944, MNRAS, 104, 273
- Booth C. M., Schaye J., 2009, MNRAS, 398, 53 (BS09)
- , 2010, MNRAS, 405, L1 (BS10)
- Boyle B. J., Terlevich R. J., 1998, MNRAS, 293, L49

- Cappellari M., di Serego Alighieri S., Cimatti A., et al., 2009, *ApJL*, 704, L34
- Cenarro A. J., Trujillo I., 2009, *ApJL*, 696, L43
- Dalla Vecchia C., Schaye J., 2008, *MNRAS*, 387, 1431
- Decarli R., Falomo R., Treves A., Labita M., Kotilainen J. K., Scarpa R., 2010, *MNRAS*, 402, 2453
- Di Matteo T., Colberg J., Springel V., Hernquist L., Sijacki D., 2008, *ApJ*, 676, 33
- Dolag K., Borgani S., Murante G., Springel V., 2009, *MNRAS*, 399, 497
- Duffy A. R., Schaye J., Kay S. T., Dalla Vecchia C., 2008, *MNRAS*, 390, L64
- Duffy A. R., Schaye J., Kay S. T., Dalla Vecchia C., Battye R. A., Booth C. M., 2010, *MNRAS*, 405, 2161
- Fabjan D., Borgani S., Tornatore L., Saro A., Murante G., Dolag K., 2010, *MNRAS*, 401, 1670
- Feoli A., Mancini L., Marulli F., van den Bergh S., 2010, *General Relativity and Gravitation*, 57
- Feoli A., Mele D., 2007, *International Journal of Modern Physics D*, 16, 1261
- Ferrarese L., 2002, *ApJ*, 578, 90
- Ferrarese L., Merritt D., 2000, *ApJL*, 539, L9
- Gaskell C. M., 2009, *arXiv:0908.0328*
- Greene J. E., Peng C. Y., Ludwig R. R., 2010, *ApJ*, 709, 937
- Gu M., Chen Z., Cao X., 2009, *MNRAS*, 397, 1705
- Häring N., Rix H.-W., 2004, *ApJL*, 604, L89
- Hopkins P. F., Hernquist L., Cox T. J., Keres D., Wuyts S., 2009, *ApJ*, 691, 1424
- Hopkins P. F., Hernquist L., Cox T. J., Robertson B., Krause E., 2007, *ApJ*, 669, 67
- Jahnke K., Bongiorno A., Brusa M., Capak P., Cappelluti N., Cisternas M., Civano F., Colbert J., Comastri A., Elvis M., Hasinger G., Ilbert O., Impey C., Inskip K., Koekemoer A. M., Lilly S., Maier C., Merloni A., Riechers D., Salvato M., Schinnerer E., Scoville N. Z., Silverman J., Taniguchi Y., Trump J. R., Yan L., 2009, *ApJL*, 706, L215
- Jarvis M. J., McLure R. J., 2002, *MNRAS*, 336, L38
- Johansson P. H., Burkert A., Naab T., 2009, *ApJL*, 707, L184
- Kisaka S., Kojima Y., 2010, *MNRAS*, 495
- Lamastra A., Menci N., Maiolino R., Fiore F., Merloni A., 2010, *MNRAS*, 537
- Lauer T. R., Tremaine S., Richstone D., Faber S. M., 2007, *ApJ*, 670, 249
- Madau P., Ferguson H. C., Dickinson M. E., Giavalisco M., Steidel C. C., Fruchter A., 1996, *MNRAS*, 283, 1388
- Magorrian J., Tremaine S., Richstone D., et al., 1998, *AJ*, 115, 2285
- Malbon R. K., Baugh C. M., Frenk C. S., Lacey C. G., 2007, *MNRAS*, 382, 1394
- McCarthy I. G., Schaye J., Ponman T. J., Bower R. G., Booth C. M., Dalla Vecchia C., Crain R. A., Springel V., Theuns T., Wiersma R. P. C., 2010, *MNRAS*, 406, 822
- McLure R. J., Jarvis M. J., Targett T. A., Dunlop J. S., Best P. N., 2006, *Astronomische Nachrichten*, 327, 213
- Merloni A., Bongiorno A., Bolzonella M., et al., 2010, *ApJ*, 708, 137
- Navarro J. F., Frenk C. S., White S. D. M., 1997, *ApJ*, 490, 493
- Nelson C. H., Whittle M., 1996, *ApJ*, 465, 96
- Peng C. Y., Impey C. D., Ho L. C., Barton E. J., Rix H., 2006a, *ApJ*, 640, 114
- Peng C. Y., Impey C. D., Rix H., Kochanek C. S., Keeton C. R., Falco E. E., Lehár J., McLeod B. A., 2006b, *ApJ*, 649, 616
- Puchwein E., Sijacki D., Springel V., 2008, *ApJL*, 687, L53
- Robertson B., Hernquist L., Cox T. J., Di Matteo T., Hopkins P. F., Martini P., Springel V., 2006, *ApJ*, 641, 90
- Salviander S., Shields G. A., Gebhardt K., Bonning E. W., 2006, *New Astronomy Review*, 50, 803
- Schawinski K., Khochfar S., Kaviraj S., et al., 2006, *Nature*, 442, 888
- Schaye J., Dalla Vecchia C., 2008, *MNRAS*, 383, 1210
- Shakura N. I., Sunyaev R. A., 1973, *A&A*, 24, 337
- Shen Y., Kelly B. C., 2009, *arXiv:0911.5208*
- Shields G. A., Gebhardt K., Salviander S., Wills B. J., Xie B., Brotherton M. S., Yuan J., Dietrich M., 2003, *ApJ*, 583, 124
- Silk J., Rees M. J., 1998, *A&A*, 331, L1
- Springel V., 2005, *MNRAS*, 364, 1105
- Springel V., Di Matteo T., Hernquist L., 2005, *MNRAS*, 361, 776
- Springel V., White S. D. M., Tormen G., Kauffmann G., 2001, *MNRAS*, 328, 726
- Tremaine S., Gebhardt K., Bender R., Bower G., Dressler A., Faber S. M., Filippenko A. V., Green R., Grillmair C., Ho L. C., Kormendy J., Lauer T. R., Magorrian J., Pinkney J., Richstone D., 2002, *ApJ*, 574, 740
- Treu T., Woo J., Malkan M. A., Blandford R. D., 2007, *ApJ*, 667, 117
- van der Wel A., Rix H., Holden B. P., Bell E. F., Robaina A. R., 2009, *ApJL*, 706, L120
- van Dokkum P. G., Whitaker K. E., Brammer G., Franx M., Kriek M., Labbé I., Marchesini D., Quadri R., Bezanson R., Illingworth G. D., Muzzin A., Rudnick G., Tal T., Wake D., 2010, *ApJ*, 709, 1018
- Vestergaard M., 2002, *ApJ*, 571, 733
- Walter F., Carilli C., Bertoldi F., Menten K., Cox P., Lo K. Y., Fan X., Strauss M. A., 2004, *ApJL*, 615, L17
- Wiersma R. P. C., Schaye J., Smith B. D., 2009a, *MNRAS*, 393, 99
- Wiersma R. P. C., Schaye J., Theuns T., Dalla Vecchia C., Tornatore L., 2009b, *MNRAS*, 399, 574
- Williams R. J., Quadri R. F., Franx M., van Dokkum P., Toft S., Kriek M., Labbe I., 2010, *ApJ*, 713, 738
- Woo J., Treu T., Malkan M. A., Blandford R. D., 2008, *ApJ*, 681, 925